Coventry University and
The University of Wisconsin Milwaukee Centre for By-products Utilization
Second International Conference on Sustainable Construction Materials and Technologies
June 28 - June 30, 2010, Università Politecnica delle Marche, Ancona, Italy.
Proceedings of Honouree sessions ed. T Naik, F Canpolat, P Claisse, E Ganjian,
ISBN 978-1-4507-1487-7 http://www.claisse.info/Proceedings.htm

Analysis on Cracking Propagation During Life of Concrete Structures Using RBSM

Hikaru Nakamura[1]

[1]*Department of Civil Engineering, Faculty of Engineering, Nagoya University*
Furo-cho, Chikusa-ku, Nagoya, 464-8603, JAPAN. E-mail: <hikaru@civil.nagoya-u.ac.jp>

ABSTRACT

The unified numerical method with structural analysis and mass transfer analysis were presented. The numerical method was applied to cracking propagation problems during the life. The thermal crack analysis in early age considering the change of material properties with cracking and the shrinkage crack analysis considering moisture transfer, creep effect and the change of material properties with cracking were presented. It was confirmed that the developed method is useful to simulate the time dependent cracking propagation.

INTRODUCTION

The sustainability of concrete structures is achieved by constructing durable concrete structures and managing adequate maintenance plan. The quality of the management depends on long-term prediction technique of the structural performance and it can be discussed only after the prediction will be done in high accuracy. The behaviour of concrete structures during the life is influenced by both time dependent behaviour due to mass transfer such as thermal, moisture transfer and chloride ions penetration and short-term behaviour due to loading such as an earthquake. Then, cracks are main factor to influence the life of concrete structures, which are also important information in maintenance procedure. For example, the thermal cracks occur at early age state and the cracks influence the durability as the initial defect. The structural performance may deteriorate due to crack occurred by the dry shrinkage and/or the corrosion of re-bars. Moreover, existence of the cracks accelerates the deterioration. Therefore, life simulation method of concrete structures focused on the cracking propagation should be developed based on the combination structural analysis with mass transfer analysis.

In this study, unified analytical method with structural analysis and mass transfer analysis is presented [Nakamura *et al*., 2006]. The Rigid-Body-Spring-Model (RBSM) is used for structural analysis and the Truss Networks model is applied for mass transfer analysis. RBSM is one of discrete approaches, which has advantage for the modeling of material discontinuity such as cracking directly relative to continuum models. The numerical method is applied to crack propagation problems during the life and the applicability is shown by the cracking propagation behavior. One is the thermal crack analysis in early age considering heat transfer and the change of material properties with cracking. Another is the shrinkage crack analysis considering moisture transfer, creep effect and the change of material properties with cracking.

STRUCTURAL ANALYSIS

Rigid-Body-Spring Model (RBSM)

RBSM, which is one of the discrete approaches, is used for structural analysis, since this method is an analytical technique based on discrete mechanics that easily deals with crack propagation of concrete directly [Saito *et al*., 1999]. RBSM represent a continuum material as an assembly of rigid particle elements interconnected by zero-size springs along their boundaries. In two dimensional model, each rigid particle has two translations and one rotational degree of freedom defined at the nuclei within. The interface between two particles consists of three individual springs in the normal, tangential and rotations, as shown in Figure 1. Since concrete cracks initiate and propagate along interparticle boundaries, the crack pattern is strongly affected by the mesh design. Therefore, random geometry using Voronoi diagrams [Bolander *et al.*, 1998] is applied to partition the material onto an assembly of rigid particle. The random geometry of the networks does not represent any structural feature within the concrete material, but rather is used to reduce mesh bias on potential crack directions.

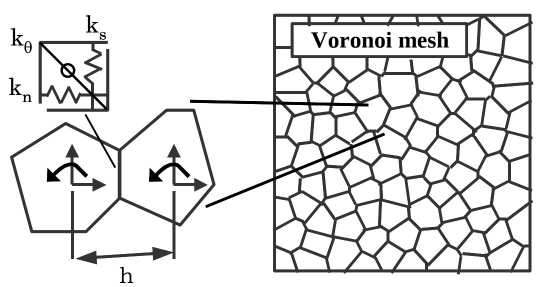

Fig. 1. Rigid-Body-Spring Networks

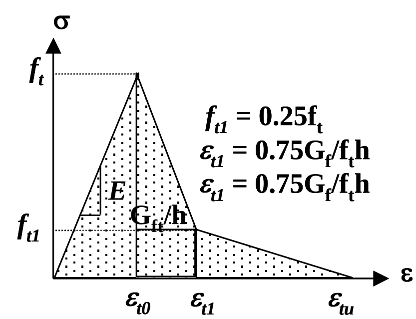

Fig. 2. Tensile behavior of concrete

Concrete Material Models for Hardened Concrete

The fracture criterion in RBSM is not based on a tensorial measure of stress, but it uses the average stresses acting normally and tangentially to the particle interface. Normal springs are set to represent the tensile and compressive strength of concrete. In this study, the tensile behavior of concrete up to the tensile strength is modeled by using a linear elastic, while a bilinear softening branch of 1/4 model is assumed after cracking, as shown in Figure 2 which is represented by the tensile strength, f_t, the tensile fracture energy, G_{ft}, and the distance between nuclei, h. In this paper, G_{ft} is set to 0.1 N/mm. The behavior under compressive strength, f'_c, is modeled using a parabolic curve up to the compressive strength.

Tangential springs represent the shear transfer mechanism of uncracked and cracked concrete. The shear strength is assumed to the Mohr-Coulomb type criterion with tension and compression caps. After shear stress reaches the yield strength, the stress moves on the yield surface until the shear strain reaches the ultimate strain.

Concrete Material Models for Early Age Concrete

The time dependent characteristics of mechanical properties of early age concrete is required to simulate thermal and shrinkage crack of early age concrete. Before cracking, elastic incremental method has been used to analyze the stress-strain behavior. On the contrast, the variation after cracking has not been defined. Therefore, in order to define the variation of concrete properties at the early age, solidification concept is applied in the constitutive model. From the analysis of the solidification process, a history integral should be used to express the rate, rather than the total value, of the strain component.

In the concept of solidification, volume equation of concrete related to the cement hydration is absolutely required. In each time step, the change of concrete strength depends on the incremental volume, $dv(t_i)$ of the previous step. Figure 3 shows the concept of solidification used in this paper [Nakamura *et al*., 2006]. Cement hydration during each time step makes solidification volume, $dv(t_i)$. Material properties depend on the volume and local stress-strain relationship is provide from the global strain, $\sigma(t_i)$ corresponding to the time i. Then, global stress, $\sigma_g(t)$ is given by the superposition all local relationship $d\sigma_g(t)$. For example, by $\varepsilon(t)$ at t_3 in Figure 3, total stress is calculated by Equation 1. The concept is simple and applicable for strain history depending on time before and after cracking. Before cracking, it shows the elastic incremental method. The local stress strain relationship is used as same as hardened concrete.

$$d\sigma_g(t) = dv(t_1)\sigma\{\varepsilon(t)\} + dv(t_2)\sigma\{\varepsilon(t)-\varepsilon(t_1)\} + dv(t_3)\sigma\{\varepsilon(t)-\varepsilon(t_2)\} \quad (1)$$

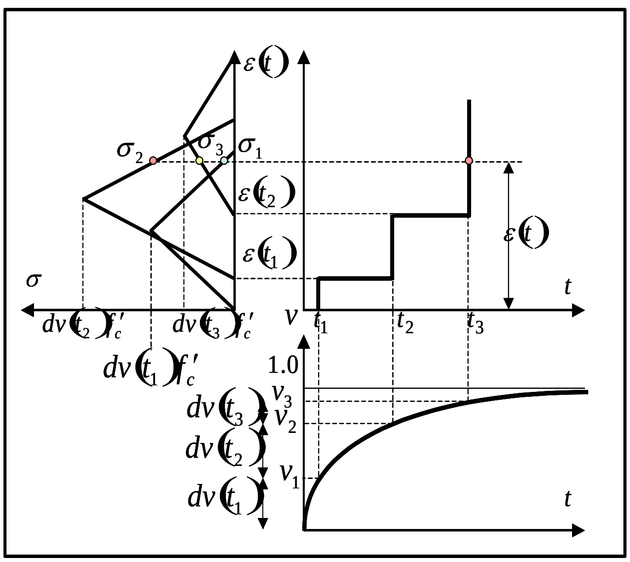

Fig.3. Concept of solidification

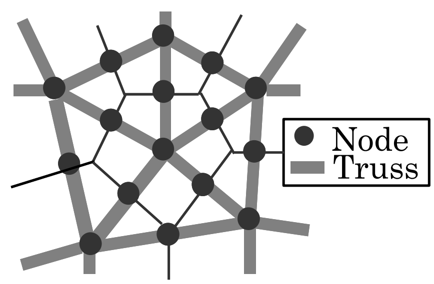

Fig.4. Truss Networks model

MASS TRANSFER ANALYSIS

Truss Networks Model

Mass transfer is a continuous flow and it is usually analyzed using the same continuum model as that use for the Finite Element approach, which is represented by a partial differential equation, whereas RBSM is used for structural analysis, which does not require continuality. The Truss Networks model is used for mass transfer analysis to obtain the initial strain for structural analysis by using RBSM with Voronoi diagrams. Each of the Voronoi elements is linked by truss elements with the nodes at the Voronoi nuclei and the intermediate points of particle boundaries, as shown in Figure 4. Then, a simplified one-dimensional diffusion equation using truss elements is employed to carry out mass transfer.

Basic Concept of Diffusion Equation

In the Truss Networks model, nonstationary potential flow problems are governed by Equation 2, a one-dimensional diffusion equation.

$$\frac{\partial \phi}{\partial t} = \frac{\partial}{\partial x}\left(D \frac{\partial \phi}{\partial x} \right) \tag{2}$$

where ϕ = some potential quantity such as the relative humidity and D = diffusivity. D is variously referred to in the case of Fourier's, Darcy's and Fick's law. Fourier's law is applied to heat transfer to simulate thermal crack, Darcy's law is applied to moisture transfer to solve drying shrinkage crack, and Fick's law is applied to chloride ion penetration.

The equation is solved by the initial condition and the following boundary condition. The boundary conditions consider all boundary surface of truss element as shown in Figure 5 even in 2-dimensional model.

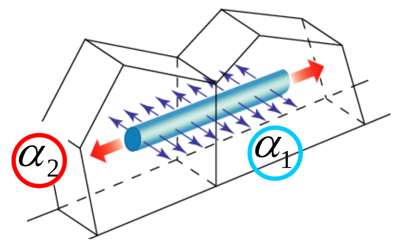

Fig. 5. Quasi-three dimensional diffusion boundary

$$\frac{\partial \phi}{\partial n} + \alpha_1 (H_s + H_0) + \alpha_2 (H_s + H_0) = 0 \tag{3}$$

where n = normal vector of drying surface, α_1 and α_2 = transfer coefficient from truss surface and truss cross section, and H_S, H_0 = some potential quantity such as the relative humidity of the drying surface and atmosphere, respectively.

UNIFICATION WITH STRUCTURAL ANALYSIS AND MASS TRANSFER ANALYSIS

Internal strain occurs in concrete due to the distribution of the mass as a result of mass transfer using Truss Networks model. In the case of drying shrinkage, a linear relationship between the change in relative humidity and the corresponding change in shrinkage strain is assumed. Then, ϕ and α in Equation 4 are represented by relative humidity and shrinkage coefficient, respectively. In the case of thermal strain, the same relationship is used in which ϕ and α are represented by temperature change and thermal expansion coefficient, respectively.

$$\Delta\varepsilon_n = \alpha \Delta\phi \tag{4}$$

Internal stress also occurs due to internal restraint from the internal strain distribution and external restraint from the boundary condition. The internal strain, $\Delta\varepsilon_n$, of each truss element obtained from mass transfer analysis is introduced to the corresponding normal springs of RBSM as structural analysis.

THERMAL CRACKING PROPAGATION

Analyzed Specimen

Thermal cracking propagation is analyzed by using the unified numerical method and the solidified constitutive model. The analyzed specimen is wall concrete structures with 300 mm and 950 mm thickness, 15000 mm lengths and 2000 mm heights[Ishikawa *et al.*,1989], as shown in Figure 6. The specimen was investigated the effect of external restraining by using the vertical reinforcement between newly concrete and hardened concrete. The reinforced bars are deformed bars with 19 mm diameter. The reinforcement ratio in vertical and horizontal are 0.767% and 0.573%, respectively. Table 1 lists the concrete properties of newly concrete at 28 days. For the specimens, Young's modulus and Poisson's ratio of hardened concrete were set to 20000 MPa and 0.17, respectively. Figure 7 shows the numerical model with 1500 Voronoi polygon meshes and the observation points A, B and C at the middle span. Points A, B and C are at 100 mm, 500 mm and 900 mm under the top surface of the newly concrete, respectively. The bottom of the hardened concrete was assumed to be roller support and the tensile strength of normal spring was set to be 0.0315 MPa, which was set to consider the weight of the structures. For heat transfer analysis, the top, left and right side surfaces are heat transfer boundary. That is, 2-dimensional heat transfer boundary is considered due to the adiabatic boundary in experiment.

Material Property

The volume function with respect to time can be derived from the Young's modulus of the experimental results, as shown in Equation 5. It should be noted that the material properties were assumed to be changed depending on age not on maturity and effective age.

$$v(t) = \frac{250t}{63 \times (4.577 + 3.799t)} \qquad (5)$$

For newly concrete, the variations of material properties such as Young's modulus, the tensile and compressive strength, and the fracture energy can be obtained by multiplying volume function and each property at 28 days based on the solidified constitutive model. It should be noted that by neglecting the creep or stress relaxation the thermal stresses may be overestimated by up to 70%. Therefore, in the analysis, the effect of creep at early age was considered simply by using correction factor of Young's modulus, $\psi(t)$ proposed by JSCE Standard[JSCE, 2002]. $\psi(t)$ = 0.73 and 1.0 for up to 3 days and after 5 days, respectively. Parameter ψ will be simply considered only in the compressive zone, since some researchers reported that the tensile creep is small when it is compared with the compressive creep.

Table 1. Concrete properties

Concrete properties	
Compressive strength, f'_c (MPa)	30.1
Tensile strength, f_t (MPa)	2.67
Young's modulus, E (MPa)	25500
Tensile fracture energy, G_{ft} (N/mm)	0.1

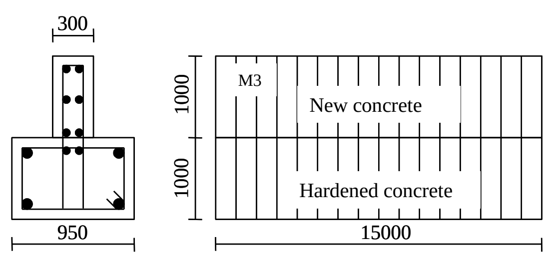

Unit: mm

Fig. 6. Outline of experiment specimens

Temperature Distribution

A time-dependent adiabatic temperature rise is assumed in order to obtain the same temperature histories with experimental results. Thermal properties of concrete are listed in

Table 2. The temperature distribution was calculated every 3 hours until 8 days. Figure 8 displays the comparison results of temperature history of points A, B and C. Truss Networks model can evaluate the temperature change and distribution reasonably.

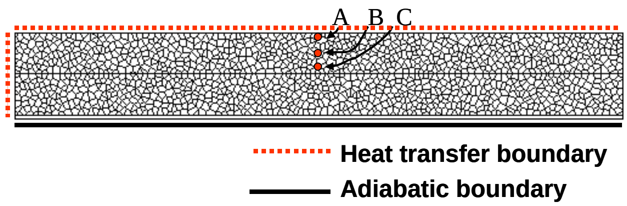

Fig. 7. Numerical model

Table 2. Thermal properties of concrete

Thermal Properties	Newly concrete	Hardened concrete
Specific heat, c (J/kg·°C)	1700	850
Thermal conductivity, k (J/m·s·°C)	6.5	7.0
Thermal convection coefficient, h (J/m^2·s·°C)	20.0	20.0
Density of concrete, ρ (kg/m^3)	2400	2400
Initial temperature (°C)	30.0	30.0
Atmosphere temperature (°C)	26.0	26.0

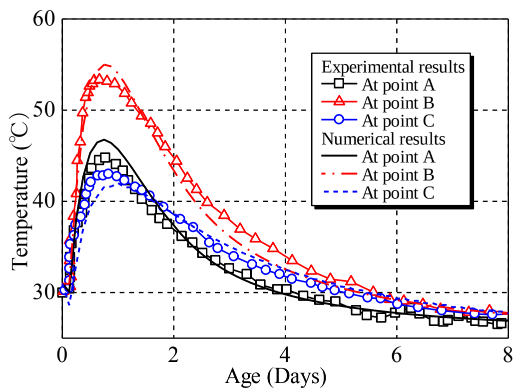

Fig. 8. Temperature history

Behavior of Specimen

Figure 9 shows the deformations, crack patterns and horizontal stress distributions of numerical results. During the increasing temperature (before 1 day), the middle span of newly concrete has compressive stresses and specimen expanded. Moreover, wall structure lift up near the both ends. When the temperature in the newly concrete passes its maximum (after 1 day), the expansion turn into contraction and horizontal stresses in newly concrete gradually change to tensile stresses. After 2 days, both ends of the wall are gradually lifted up and tensile stresses gradually increase. Until 4 days, main crack occur near the middle span. After that main crack continuously grow and propagate in the upward and downward direction at the same time and crack width gradually increase as well. At 5.5 days, through crack occur and crack width suddenly spread out. Horizontal stresses that are adjacent to this crack abruptly decreased. As the results, the position of crack, cracking dates and crack propagations are similar to the experimental one and cracking behavior can be clearly seen step by step. These are the merit of the proposed model.

Figure 10 shows the comparison results of stress histories between experimental and numerical results of points A, B and C. As the results of point A, stresses of the numerical are higher than the experimental, since the difference of aging for each element due to temperature gradient and history does not consider. However, the suddenly decreasing of horizontal stresses after through crack occurring can be clearly observed in the analysis at 5.5 days. As mentioned before, elastic incremental method has been normally used to analyze the behavior of early age concrete before cracking. Therefore, to clearly show the different between elastic incremental method and the solidified constitutive model, the specimen is calculated by using elastic incremental method and display in Figure 11. As can be seen, horizontal stresses obtained from elastic incremental method show the different results to the experimental ones because the elastic incremental method cannot consider the effect of microcracks. These points are the advantages of the solidified constitutive model. Moreover, the suddenly decreasing of horizontal stresses after through crack occurring could not be observed as well.

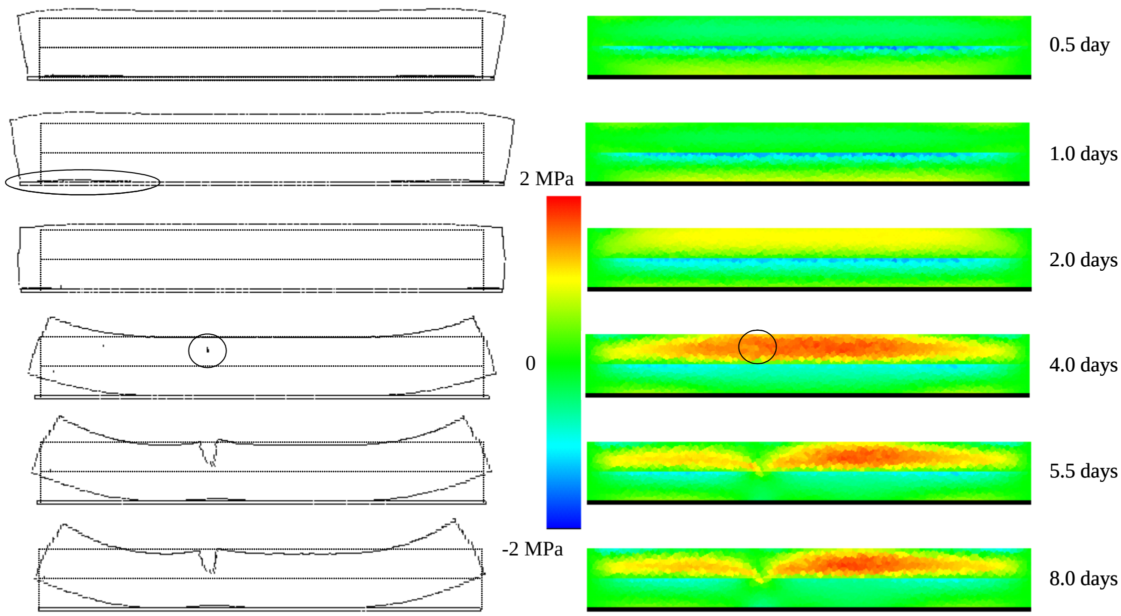

a) Deformations and Crack patterns. b) Horizontal stress distribution.

Fig. 9. Behavior of wall structure

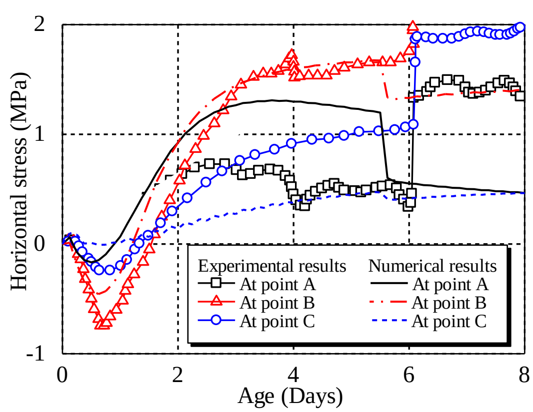

Fig. 10. Horizontal stresses at middle span (Solidified constitutive model)

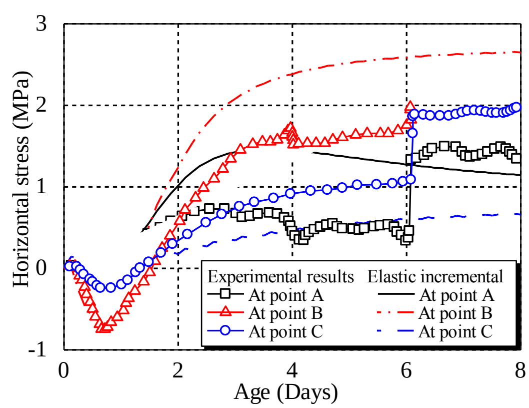

Fig. 11. Horizontal stresses at middle span (Elastic incremental method)

DRYING SHRINKAGE CRACKING PROPAGATION

Analyzed Specimen

Crack propagation analysis due to drying shrinkage is performed for the uniaxial restrained drying shrinkage test carried out by Kojima *et. al.* [Kojima *et. al*., 1993]. Figure 12 shows the outline of test specimen which is the standard size of the test specimen (160 x 100 x 1000 mm) of Japanese Industrial Standard (JIS). The numerical model with 1000 Voronoi elements is generated. The element sizes of about 10mm are generated in the bottleneck area. For boundary condition of structural analysis, vertical displacement at the bottom of the specimen and horizontal displacement at the both ends of the specimen are fixed. The moisture boundaries for moisture transfer analysis are set uniformly along the bottleneck area, at the both ends of the specimen and on the both surface of specimen using quasi-three dimensional diffusion boundary. Relative humidity measured during test is introduced directly in the analysis as conditions of atmosphere. Note that irreversibility of wet and dry is not considered in the analysis.

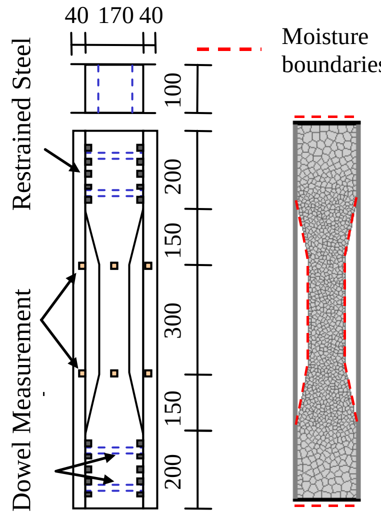

Fig. 12. Outline of test specimen and model

Material Property

The volume function with respect to time can be derived considering the experimental results of tensile strength at 90 days, as shown in Equation 6. The compressive strength, tensile strength and Young's modulus of concrete at 90 days are 28.2 N/mm^2, 2.82N/mm^2 and 23400 N/mm^2, respectively

$$v(t) = \frac{3.224 \cdot t}{20 + t} \tag{6}$$

In the analysis, the variations of material such as Young's modulus, tensile and compressive strength and fracture energy can be obtained by multiplying volume function and each property at 90 days based on the concept of modified solidification. Poisson's effect of concrete is not considered in the analysis.

The effect of creep at early age is considered by Equation 7. The creep strains in normal springs and shear springs of RBSM are calculated by step-by-step method, in which internal stress increment of the each spring is evaluated in every step,

$$\varepsilon_{cr}(t_m) = \sum_{i=1}^{m-1} \phi(t_m, t_i) \Delta\sigma_i \qquad (m \geq 2) \tag{7}$$

where t_i is time, $\varepsilon_{cr}(t_m)$ is total creep strain at t_m and $\phi(t_m, t_i)$ is creep function which is defined as creep strain during $(t_m - t_i)$ subjected to unit stress applied at t_i . $\Delta\sigma_i$ is incremental stress from t_{i-1} to t_i. In this study, it is assumed that properties of compressive and tensile creep are the same. The creep function was identified by analyzing for creep test specimen (100 x 100 x 500 mm) which had been tested under compressive stress about 6MPa without restrained and is derived as Equation 8.

$$\phi(t,t_i) = \frac{0.39}{E(t_i)}(t - t_i)^{0.35} \tag{8}$$

For the moisture diffusivity, the relationship dependent on moisture content is applied as expressed as Equation 9, which is proposed by Bazant and Najjar [Bazant and Najjar, 1972].

$$\frac{D}{D_1} = \alpha_0 + \frac{1-\alpha_0}{1+\left(\frac{1-R}{1-R_c}\right)^n} \tag{9}$$

where D_1 is initial diffusivity and R is moisture content. Each parameter is set as 0.05 for α_0, 0.75 for R_c and 16 for n, respectively.
The moisture diffusion properties of concrete are shown in Table 3 which were identified by parametric analysis of free drying shrinkage test (size of specimen was 100 x 100 x 500 mm).

Table 3. Parameter for moisture transfer

Parameter	Value
Moisture diffusivity within bulk concrete, D (mm^2/day)	30.0
Water transfer coefficient, α_1 (mm/day)	0.1
Water transfer coefficient, α_2 (mm/day)	1.5
Shrinkage coefficient, α (mm/day)	0.0027

Behavior of Specimen

4 types of analytical case are performed in order to clarify the effectiveness of each model. In case 1, only drying shrinkage is analyzed without considering the effect of creep and material properties changing. In case 2 and 3, creep model and solidification concept are considered in addition to case 1, respectively. In case 4, both of creep model and solidification concept are combined to case 1.

Figure 13 shows the shrinkage strain for each case. The specimens gradually shrink with an increasing of times until through crack occurring and it corresponds the time when strain changes to be negative value drastically. After the points, tensile strain gradually increase. The times corresponding to through crack occurring are influenced by the combination with the change of material properties and creep effect.

Figure 14 shows the crack pattern of case 4 at 52, 82, 85 105 and 145 days. At 52 days, many micro cracks are observed at the bottleneck region because of the internal restraint due to moisture transfer. The micro cracks increase and progress inside the specimen at 82 days. As can be observed, when through crack occur at 85 days, micro cracks at the bottleneck region close because internal restraint decrease and tensile stresses are released. Finally, through crack develop and crack width increase. It is confirmed that cracking behavior such as crack occurrence and propagation of uniaxial restrained concrete under drying shrinkage specimen can be simulated by the analytical model.

Figure 15 displays the comparison of crack width between experimental and numerical results. For every case, crack width spread suddenly and gradually increase with an increase of times which has the same behavior as experiment. Crack width just after through crack occurring of case 3 and 4 are larger than that of case 1 and 2. This is because that strain at the macroscopic tensile strength increases according to the effect of the solidification concept. Since the specimen after through crack occurring is not restrained and behave as the same with free drying shrinkage, the increase of crack width of every numerical result after through crack occurring are similar to that of experimental result. In the result of case 4, it can be seen that crack propagation behavior is almost the same with experiment, in terms of crack occurrence, crack development and crack width. It is confirmed that the analytical method with the solidification concept and the creep model is effective to evaluate the crack propagation behavior due to drying shrinkage.

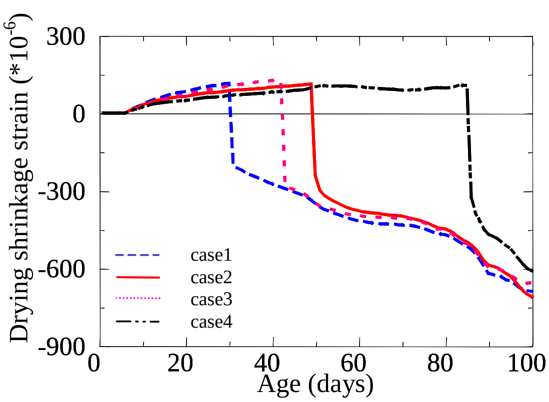

Fig.13. Drying shrinkage strain

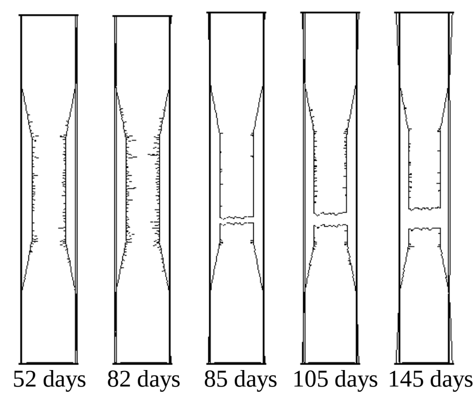

Fig.14. Crack pattern

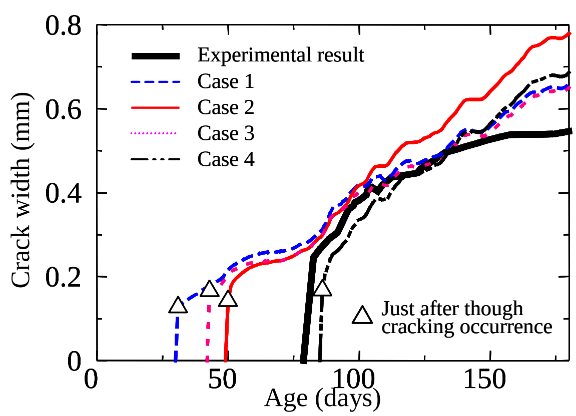

Fig.15. Change of crack width.

CONCLUSIONS

A time-dependent analytical model to analyze mass transfer and cracking behavior was developed. The Rigid-Body-Spring Model was used for structural analysis and the Truss Network model was utilized for mass transfer analysis. As the mass transfer, Thermal transfer and moisture were adopted. Then, the cracking propagation behavior of thermal stress and drying shrinkage were simulated. The analysis was found to simulate well cracking propagation considering the solidification concept of material properties and creep behavior.

Therefore, the method is useful to predict cracking propagation behavior during the life of concrete structures.

REFERENCES

Bazant, Z.P. and Najjar, L. J. (1972) “Nonlinear Water Diffusion in Nonsaturated Concrete.” *Materials and Structures*, 5(25), 3-20.

Bolander, J.E. and Saito, S., (1998) "Fracture analysis using spring networks with random geometry." *Engineering Fracture Mechanic*, 61, 569-591.

Ishikawa, M., Maeda, T., Nishioka, T., and Tanabe, T. (1989) “An Experimental Study on Thermal Stress and Thermal Deformation of Massive Concrete.” *Proceedings of JSCE*, 11(408), 121-130.

JSCE, (2002). “Standard Specifications for Concrete Structure-Structural Performance Verification.” Tokyo, Japan Society of Civil Engineers.

Kojima, M., Suzuki, K., Ohno, Y. and Nakagawa, T. (1993) “Cracking Tendency of High Early Concrete Range Water Reducing Agent.” *Proceedings of the Japan Concrete Institute*, 15(1), 429-434 (in Japanese).

Nakamura, H., Srisoros, W. Yashiro, R. and Kunieda, M. (2006) “Time-Dependent Structural Analysis considering Mass Transfer to Evaluate Deterioration Process of RC Structures.” *Journal of Advanced Concrete Technology*, 4(1), 147-158.

Nakamura, H., Srisoros, W. and Kunieda, M(2006) "New structural analysis considering deterioration process induced by mass transfer", *International Journal of restoration of buildings and monuments*, Vol.12,No.4, 317-334.

Saito, S. and Hikosaka, H. (1999) “Numerical analyses of reinforced concrete structures using spring networks models.” *Journal of Materials, Concrete Structures and Pavements*, JSCE, 672(44), 289-303.